



# IDENTIFICATION OF NOVEL MUTATIONS IN THE CDKN1B GENE IN INVASIVE CARCINOMA OF BREAST

Amania Anwar, Sheeba Murad, Summer Gul, Rehan Zafar Paracha, Amjad Ali  
Atta-ur-Rehman School of Applied Biosciences,  
National University of Science and Technology,  
Islamabad, Pakistan

Peter Bloodsworth  
School of Electrical Engineering and Computer Sciences,  
National University of Science and Technology,  
Islamabad, Pakistan

**Abstract**— Cyclin dependent kinase inhibitor p27Kip1 (also known as CDKN1B) is an atypical tumor suppressor implicated in cell cycle regulation, proliferation and differentiation. Although, the impaired p27Kip1 protein expression and mislocalization is anticipated in various cancers, however, it is rarely reported to be mutated. We report novel mutations: c.4\_6insGTT and c.520delA in Kip1 gene, cloned from an invasive ductal carcinoma patient. The protein sequence analysis revealed c.4\_6insGTT resulted in addition of valine at codon 2. Whereas, c.520delA mutation lead to frameshift mutation that altered entire series of codon followed by codon 173. By protein-protein interactions, we found mutations altered the distance between ATP binding pocket of AKT1 with p27Kip1 phosphorylation sites. In addition, electrostatic potential maps showed an excessive distribution of positive charges at C terminal end. Collectively, the analysis of the effect of these mutations on the protein function might provide molecular insight for future treatments.

**Keywords**- Akt1, ATP binding pocket, Phosphorylation sites, Protein-protein interactions. Invasive ductal carcinoma, p27<sup>Kip1</sup>

## I. INTRODUCTION

P27<sup>Kip1</sup>, a cyclin dependent kinase inhibitor (CDKIs) negatively regulates eukaryotic cell cycle<sup>1</sup>. It binds and inhibits the kinase activity of cyclins-cdk complexes which arrests cell cycle progression from G1 to S phase<sup>2, 3</sup>. Thus, p27<sup>Kip1</sup> acts as a tumor suppressor and any alteration in its function could trigger tumorigenesis<sup>4</sup>. The intrusion of p27<sup>Kip1</sup>

protein in the pathogenesis of invasive ductal carcinoma, either by loss of p27 protein expression or inactivation of its activity via mutation has been focused in several studies. In breast carcinoma, low p27<sup>Kip1</sup> protein level is associated with higher cell proliferation and histological grade<sup>5, 6</sup>. Nevertheless, P27<sup>Kip1</sup> gene mutation and allelic losses are uncommon in breast cancers<sup>7</sup>. Considering the importance of p27<sup>Kip1</sup> as a potent tumor suppressor we were interested to explore p27<sup>Kip1</sup> gene mutations in invasive ductal carcinoma. Hereby, we report a novel p27<sup>Kip1</sup> mutation, found in an invasive ductal carcinoma patient from Pakistan. Combining sequencing analysis, protein modeling, protein-protein interactions and electrostatic charge distribution, we predict the probable implication of these mutations in oncogenesis.

## II. METHODOLOGY

### A- RNA Extraction and Cloning –

A 60 year old female was diagnosed with invasive ductal carcinoma with no family history of cancer. On laboratory examination, the tumor was estrogen, progesterone and Human epidermal growth factor 2 (Her2) receptor negative. The malignancy was found to be of grade II with metastasis in lymph nodes. Fresh breast cancer biopsy sample was collected after a patient's consent. Total RNA was extracted with Trizol reagent (Invitrogen, Carlsbad, CA) according to manufacturer's protocol. Sequence specific primers were designed from CDKN1B sequence retrieved from NCBI database. The sequences of the primers were forward primer GGATCCACCATGGTTTCAAACGTGCGAGTGT and Reverse primer CTCGAGGAGCTGTTTACGTTTGACGTCTTCTGA. Extracted RNA was then used as a template for cDNA



synthesis. Initially, 11 $\mu$ l of RNA and 1 $\mu$ l of Oligo(dT)18 primer (Fermentas) was diluted with DEPC water up to 12.5 $\mu$ l and kept at 70 degrees for 5min and then on ice for 5 min. Later, 2 $\mu$ l of (10Mm) dNTPs, 4 $\mu$ l of 5x RT Buffer, 0.5 $\mu$ l of RiboLock Tm RNase inhibitor and 20 units of RevertAid Tm reverse transcriptase enzyme (Fermentas, Canada) were added to the reaction mix. Final volume was 20 $\mu$ l and the cDNA synthesis was carried out at 42 degrees for 60 minutes, followed by 70 degrees for 10 minutes. CDKN1B gene was amplified using conventional PCR. The PCR reaction mix contained 3 $\mu$ l of cDNA as template, 10 pmol each of Forward and Reverse primer, 2 $\mu$ l of (2mM) DNTPs, 2 $\mu$ l of (25mM) MgCl<sub>2</sub>, 2 $\mu$ l of 10X of Taq buffer (Fermentas, Canada), 40 units of Taq polymerase and nuclease free water to make up the volume. The cycle conditions for PCR were as follows: Initial denaturation step at 95°C for 5 minutes, followed by 35 cycles of first denaturation step at 94°C for 40 seconds, annealing at 58°C, 30 minute and extension at 72°C for 30 seconds. The final extension was carried at 72°C for 10 minutes. As expected, 615 base pair band was observed when the PCR product was checked on 2% agarose gel. Amplified CDKN1B gene was purified by silica bead gel extraction kit (Fermentas) according to manufactures protocol. The purified PCR product was cloned in TA vector (Thermo Scientific: Inst TA cloning kit). In short, 19 $\mu$ l of PCR product was mixed with 6 $\mu$ l of 5 x ligation buffers, 1 $\mu$ l of T4 DNA ligase, 3 $\mu$ l of TA vector and 1 $\mu$ l of nuclease free water. The ligation mix was kept at 4 degrees overnight and later was transformed into DH5  $\alpha$  cells by the heat shock method. Initially, the transformed cells were subjected to blue, white selection and then positive clones were screened by restriction digestion

### **B. Sequencing and Mutational Analysis –**

Three clones of the sample were sent for sequencing to Sure BioDiagnostics, Karachi, Pakistan. Sequencing was carried out both from sense and antisense primers and sequence was submitted in Genebank (<http://www.ncbi.nlm.nih.gov/genbank>) with an accession number JX628784. All existing human CDKN1B protein sequences were retrieved from Uniprot (<http://www.uniprot.org/>) and were aligned to generate a wild type consensus sequence by CLC work bench ([www.clcbio.com](http://www.clcbio.com)). The wild type protein sequence was aligned with our generated sequence and then the sequence was analyzed for probable mutations. Later, C terminal end of the wild type p27 protein sequence was aligned with sequences of CDKN1B orthologs present in uniprot (ID no: H2Q5H2, P46414, Q6SLL5, O19001 and Q8JIV2).

### **C. Protein structure Modeling-**

Protein sequences of CDKN1B (ID no.P46527) and AKT1 (ID no. P31749) were retrieved from Uniprot database. Sequences

were submitted to NCBI provided protein specific iteration (PSI)-BLAST tool (<http://blast.ncbi.nlm.nih.gov/Blast.cgi>) to obtain homologous sequences of three dimensional structures available in protein data bank (PDB).

Two PDB structures, including PDB codes: 1JSU (Crystal structure of p27<sup>Kip1</sup> cyclin dependent kinase inhibitor bound to the cyclin A-Cdk2 complex determined at 2.3Å)<sup>8</sup> and 3O96 (Crystal structure of human Akt1 with an allosteric inhibitor resolved at 2.7Å)<sup>9</sup> have a maximum sequence identity with P27<sup>Kip1</sup> and Akt1 respectively. So for the complete 3D structure of p27<sup>Kip1</sup> protein the structure was built using ab-initio modeling techniques. P27<sup>Kip1</sup> protein sequence was submitted in I-TASSER (Iterative threading assembly refinement)<sup>10</sup> and Phyre2 (Protein Homology/analogy Recognition Engine V 2.0)<sup>11</sup>. I-TASSER (<http://http://zhanglab.ccmb.med.umich.edu/I-TASSER/>)

construct models by reassembling continuous fragments excised from homologous templates generated via multiple threading program. Models generated by these software's were evaluated by online servers such as ERRAT, PROCHECK, QMEAN and Z score<sup>12, 13</sup>. However, all models showed low ERRAT, QMEAN and Z scores. In Ramachandran plot, most of the residues were found in unfavorable regions. P27<sup>Kip1</sup> sequence was submitted in ab initio modeling servers such as QUARK and ROSETTA (<http://rosetta.bakerlab.org/>). QUARK build low to high resolution structures by assembling continuous fragments (1-20 residues) retrieved from unrelated protein structures. However, ROSETTA combines template based homology modeling with ab initio methods. Multiple models were generated and one target model was selected with highest ERRAT and QMEAN scores, least Z score and with favorable Ramachandran plot statistics. Mutated model was generated using the finest model obtained in earlier steps. The modeling of mutated model was performed using homology modeling program MODELLER<sup>14</sup>. The energy minimizations were performed in Molecular modeling and simulation (MOE) software (Chemical computing group's MOE software, version 2013) and then analyzed using the same criteria as were used for a wild type model of P27<sup>Kip1</sup> (Nmp27). Apo-AKT1 model was derived from Human Akt1 bound with an allosteric inhibitor (PDB ID no. 3O96) using MOE.

### **D. Protein-protein interaction of Akt1 and P27<sup>Kip1</sup>**

Protein protein interactions of both non-mutated and mutated models of P27<sup>Kip1</sup> (termed as Nmp27 and Mp27, respectively) were studied by using High Ambiguity Driven Molecular Docking web server (HADDOCK) ([haddock.science.uu.nl](http://haddock.science.uu.nl))<sup>15</sup>. The webservice generates 10 clusters. Scoring is based on Haddock score, desolvation energy, Z score, RMSD value, electrostatic energy, buried surface area, restrains violation energy and van der Waals energy. Possible active and passive residues of of Nmp27, Mp27 and Akt1 were predicted by CPORT (Consensus Prediction Of interface Residues in



Transient complexes) webserver<sup>16</sup> and were integrated in haddock program. Haddock server predicted most probable protein- protein interaction interfaces (PPI) between Nmp27-Akt1 and Mp27-Akt1. The best complexes were selected with the least Haddock score. Additionally, the distance between the Akt1, ATP binding pocket GKGTFG<sup>17</sup> and phosphorylation sites within Mp27 and Nmp27 were determined by pymol (v1.3). Further Delphi<sup>18</sup> was used for calculating electrostatic charges on the surface of Nmp27, Mp27, Nmp27-Akt1 and Mp27-Akt1 protein complexes.

### III. RESULTS

#### A-Cloning, sequencing and Mutational analysis

In order to confirm the positive clones with CDKN1B gene, extracted plasmids were restricted digested with EcoRI( Fast digest: Fermentas) and BamHI (Fast digest: Fermentas) restriction enzymes and analyzed on 1% agarose gel, represented in supplementary Figure 1a. An insertion of 3 nucleotides; GTT was found at position 4-6 nucleotides (c.4\_6insGTT as shown in supplementary Figure 1b). This insertion mutation resulted additional hydrophobic residue valine at the second position of p27<sup>Kip1</sup> protein shown in Figure 1a. Moreover, there was no change in the secondary structure elements at this site of mutations. Moreover, a deletion of a single nucleotide Adenine was found at 520th position (c.520delA as seen in supplementary Figure 1b), which implicated a frame shift mutation at C terminus and resulted in alteration of entire reading frame as shown in Figure 1a. In addition, an Akt1 phosphorylation site RKRPAT present at its nuclear localization sequence (NLS; amino acids 151–166) remained unaltered. In addition, B hairpins (61-71), B strand (75-81) and helix (residues 85-90) which interact with Cdk2 and the LFG motif which binds with cyclin A all remained unchanged. Wild type amino acid residues following from 174th position NVSDGSPNAGSVEQTPKKPGLRRRQT were replaced by MFQTVQPMPVLWSRRPRSLASEDVKR amino acid residues (Figure 1a). Interestingly, this mutated region at C terminus was found to be conserved in all p27 orthologs other than *Mus musculus* and *Gallus gallus* whereas N terminus was conserved in all species (Figure 1b).

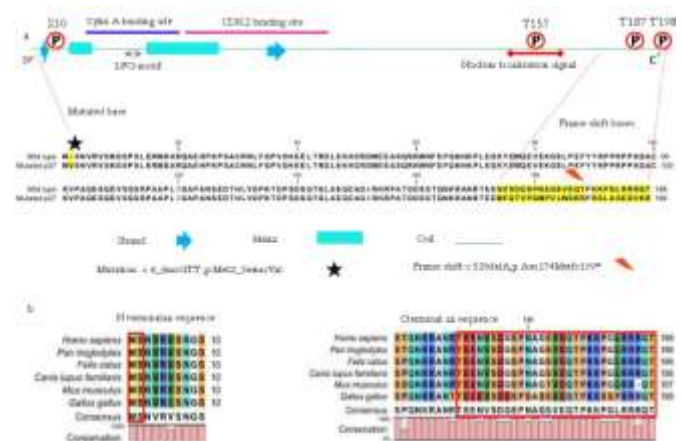


Fig. 4. Multiple-sequence alignment of p27kip1 protein with functional regions (a) Predicted secondary structure elements for p27 Kip1 protein shown by strand, helix and coil and important regions in p27 Kip1 protein are represented: phosphorylation sites Ser10, T157, T187 and T198, Cyclin A binding domain, LFG motif, CDK2 binding site, Nuclear Localization signal. Sequence alignment of the wild type and mutated p27 Kip1. Uncolored residues are identical in both. Mutated residues are highlighted with yellow color. (b) Highly conserved consensus sequence of N and C terminal ends of p27 Kip1 orthologs.

#### B- Protein Structural Modeling

Protein sequence of CDKN1B which was submitted in (PSI)-BLAST facility showed 80% sequence identity with P27 (PDB codes: 1JSU). However, this structure lacked complete query coverage and our interest areas: N and C terminus. Webserver QUARK and ROBETTA generated fifteen 3D models for complete P27<sup>Kip1</sup> protein. Model 4 generated from ROBETTA was rated as the best model on the basis of ERRAT, Rampage and QMEAM scores. PROCHECK-based Ramachandran map statistics found 87.8 % of Model 4 amino acid residues in the favored region, 11% in the additionally allowed region and only 0.6 % residues in the disallowed region. These results indicate that this model has protein structure with favorable stereo-chemical property<sup>13</sup>. Moreover, Z score was found to be -2.97 and the Qmean score of 0.488. After refinement of predicted residues present in disallowed regions, the overall quality factor of the *ab initio* model was 90.86 % in the ERRAT plot and it showed few atomic attractions creating steric hindrance between amino acids which are represented in Figure 2.

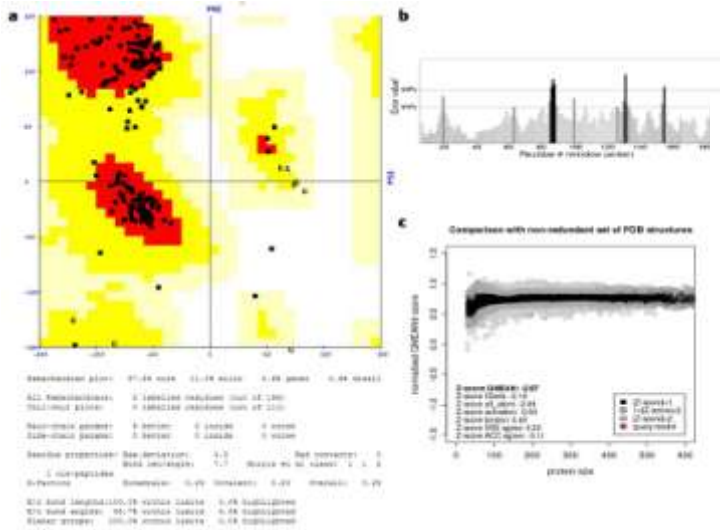


Fig. 2. Evaluation of model 4. a PROCHECK based Ramachandran map, b ERRAT plot, c Q-mean Z-score plot.

Protein –protein interactions of Akt1 and P27<sup>Kip1</sup>

P27<sup>Kip1</sup> was docked with Akt1 via Haddock web server, 145 water refined complexes were generated, grouped in 10 clusters. The Haddock score, buried surface area, Z score, RMSD, Electrostatic energy, Cluster size, van der waals energy, desolvation energy, restrains violation energy for all the clusters are shown in Figure 3. A complex of p27<sup>Kip1</sup> and Akt1 with a haddock score of  $-71.5 \pm 10.2$  was selected as the best probable complex. Further, Haddock predicted 147 water refined complexes for Mp27 and Akt1. Cluster 2 was rated as the best complex with a Haddock score of  $-138.4 \pm 10.1$  and the rest of the criterion generated by haddock are represented in Figure 4.

Fig. 3. (a) Graphical representation of scores generated by Haddock for clusters 1-10

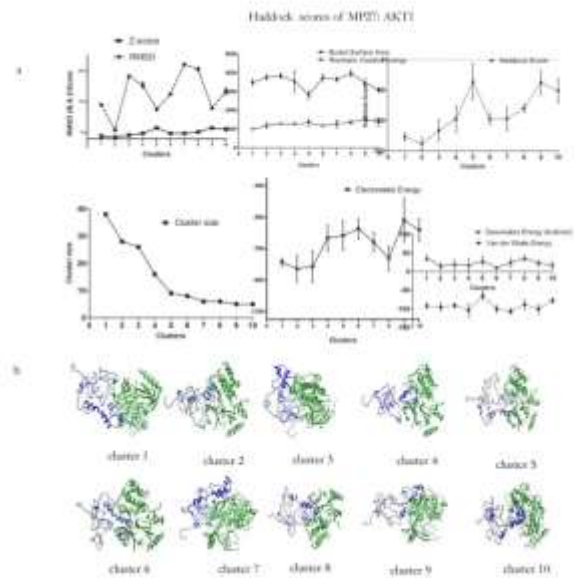


Fig. 4. (a) Haddock generated scores of protein protein interaction (PPI) between mutated p27 and AKT1. (b) Cartoon representation of complexes 1-10 (MP27: AKT1) generated by Haddock, mutated P27 highlighted in blue and AKT1 in green colour

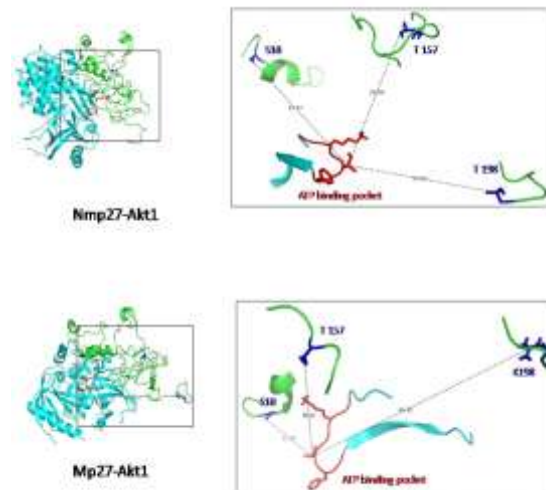
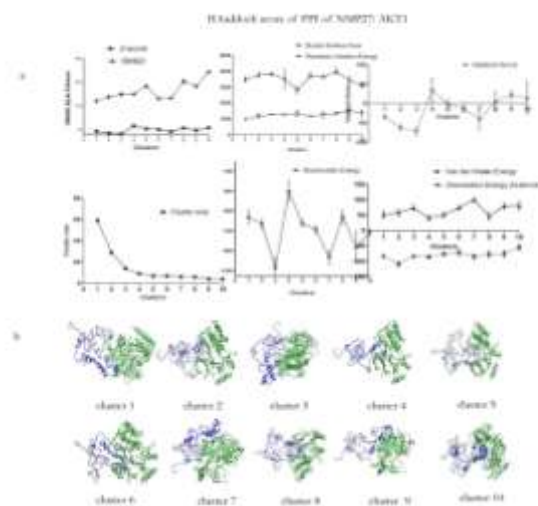


Fig. 5. Ribbon representation of Nmp27 and Mp27 protein structures bound with Akt1 shown. Structural analysis revealed varied distance between Akt1 (ATP binding pocket) and Akt1 phosphorylation sites: T198, T157, and K198, T157, S10 of Nmp27 and Mp27 respectively.

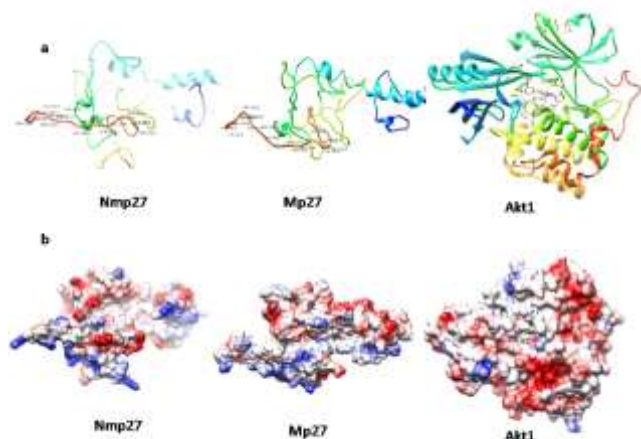


Fig. 6. Structural models and electrostatic potential maps of non-mutated p27kip1, mutated p27kip1 and Akt1. (a) Altered amino acids at C terminal are shown in non-mutated and mutated p27kip1 protein models. Human AKT in complex with an allosteric inhibitor (shown in sticks) bind with human Akt1 into the deep ATP-binding cleft. (b) Electrostatic potential maps on the surface of residues for all structures. It is demonstrated that in non-mutated p27 model the C terminal region is somewhat mixture of negatively and positively charged residues, whereas in mutant model the coulombic surface is showing a trend of positively charged regions. Akt1 demonstrates even distribution of coulombic charges (Blue positive charges, red negative charges).

Additionally, the distance between the Akt1 (ATP binding pocket GKGTFG)<sup>17</sup> and phosphorylation sites within Mp27 and Nmp27 were determined by pymol (v1.3). Interestingly the distance for S10 phosphorylation site for mutated p27<sup>Kip1</sup> decreased, however the distance between T157 and ATP binding pocket increased shown in Figure 5.

Further, electrostatic potential maps were used to illustrate charge distribution on the surface of Akt1 (Figure 6), Nmp27, Mp27 and their complexes. In non-mutated model (Nmp27), negative (depicted by red color) and positive charges (blue color) were uniformly distributed at its C terminal (Figure 6). However, in Mp27 the positively charged surfaces were more in comparison with negative charges at its mutated C terminal.

#### IV. DISCUSSION

p27<sup>Kip1</sup> is known as tumor suppressor, mediator of apoptosis, a regulator of cell cycle and cellular differentiation<sup>19</sup>. There are growing numbers of reports demonstrating the oncogenic potential of various genetic mutants of tumor suppressive genes/ cell cycle regulators. However, unlike some genes such as the p15 and p16, mutations in p27<sup>Kip1</sup> gene seem to occur rarely<sup>20</sup>. Two different mechanisms have been implicated in p27<sup>Kip1</sup> inactivation during tumour development: its nuclear export and enhanced protein degradation Shin<sup>21</sup>. During G1-S transition, p27 is actively phosphorylated at Thr187 by cyclin E-CDK2<sup>22</sup>. Thr187-phosphorylated p27<sup>Kip1</sup> is recognized by Skp2-containing E3 ubiquitin ligase, Skp, Cullin, F-box

containing complex (SCF complex) and its cofactor, Cdk subunit1 (Cks1) which promote its degradation by proteasome<sup>23</sup>. However, the sub cellular localization of p27<sup>Kip1</sup> is dependent on the phosphorylation of three key amino acid residues S10, T157, T198 by Akt1. Mutation at T157 impedes AKT1 induced phosphorylation and promotes its nuclear localization. A complete reversion of AKT1 induced cytoplasmic re-localization was demonstrated in the presence of double mutation at T157A and T198A<sup>24</sup>.

In this study, we report novel mutations found in p27<sup>Kip1</sup> mRNA isolated from invasive ductal carcinoma patient. Firstly, there was an addition of GTT nucleotides at position 4-6 in the coding sequence which lead to an addition of valine a hydrophobic residue at codon 2. The concept of kozak consensus sequence GCCRCCaugG (where R = purine and "aug" is the initiation codon), with the -3R and +4G being particularly important for translation initiation. Kozak<sup>25</sup> found +4G enhances translation initiation, but does not when it occurs in a GUN codon (coding for valine). Another study in Escherichia coli demonstrated consistent findings that valine at penultimate site (second position) reduces initiator Met cleavage in comparison with amino acids such as Ala, Cys, Gly, Pro, or Ser<sup>26</sup>. In contrast, few studies on prokaryotes and eukaryotes propose that cleavage of Met occurs with valine at this position<sup>27</sup>. Kozak consensus sequence is not the only criterion which initiates translation thus any outcome of this mutation cannot be predicted until further validation. In addition, a deletion of a single nucleotide Adenine was found at 520th position in the coding sequence, which implicated a frame shift mutation at C terminus and resulted in alteration of the entire reading frame. Wild type amino acid residues following from 174<sup>TH</sup> position which were NVSDGSPNAGSVEQTPKKPGLRRRQT were replaced by MFQTVQPMPVLWSRRPRSLASEDVKR amino acid residues. This C terminal region was found conserved in all p27<sup>Kip1</sup> orthologs other than mouse and chicken thus implying its significance in p27<sup>Kip1</sup> functionality. These mutations have been reported for the first time. Although Norihiko et al and M. Veronica Ponce-Castaneda et al in independent studies found neither deletions, nor rearrangements in p27<sup>Kip1</sup> gene when screened in various solid tumors<sup>28, 29</sup>. Besides a hemizygous deletion in p27<sup>Kip1</sup> was found in a B-cell non-Hodgkin's lymphoma<sup>29</sup>. In adult T-cell leukemia, a stop codon mutation at 76 was found<sup>29</sup>. In addition two point mutations were found during 36 primary breast carcinomas. One of the mutations in the breast carcinomas was a polymorphous mutation at codon 142 and the other a nonsense mutation at codon 104<sup>7</sup>.

Recent advances in computational methods provide insights into the effect of mutations on protein structure and make it plausible to interpret its interactions with other proteins. In this study we have used in silico tools to model non mutated and mutated p27<sup>Kip1</sup>. The reliability of the protein models were evaluated on several parameters including by ERRAT, Ramachandran, Qmean and Z score. Where, 90.86% ERRAT,



-2.97 Z score with 0.488 Qmean score. The final p27 model which was selected had bond angles, lengths, dihedrals and interaction energy within the allowed range without atomic clashes. These results supported the use of this model as a template to model mutated p27, followed by protein-protein interactions (PPIs) of P27<sup>Kip1</sup> with Akt1. The predicted models of Nmp27 and Mp27 showed no structural difference relative to each other. Protein-protein interactions play a vital role in various biological processes including signal transduction, cell metabolism and muscle contraction<sup>30</sup>. However, experimental analyses of PPIs have certain limitation such as a need to anticipate the likelihood of interactions before initiating an experiment. Therefore, computational tools can blindly predict binding interfaces between proteins. In our study Haddock tool was used to predict most probable PPIs interfaces for Nmp27- Akt1 and Mp27- Akt1 with a haddock score of  $-71.5 \pm 10.2$  and  $-138.4 \pm 10.1$ . Electrostatic interactions are non-covalent interactions, which occur between electrically charged atoms having both positive and negative interactions<sup>31</sup>. It plays a key role in determining the nature and strength of the PPIs. Here electrostatic potential maps of Akt1, Nmp27, and Mp27 were determined. Akt1 and Nmp27 show even distribution of positive and negative charges. However Mp27 demonstrated excessive positive charges at its mutated C terminal. Thus, it is most likely that Mp27 binds less strongly with Akt1 in comparison with Nmp27 due to electrostatic repulsion. Further, whether a C terminal frameshift mutation had any effect on the remaining Akt1 phosphorylation sites: S10 and T157 were determined by measuring distance between the phosphorylation site and ATP binding pocket (GKGTFG)<sup>17</sup>. The distance of S10-Akt1 decreased from 32.3Å in Nmp27 to 11.35Å in Mp27. Moreover, the distance of T157-Akt1 changed from 26.8Å to 38.2Å due to mutation.

## V. CONCLUSION

In conclusion, T198 and T187 phosphorylation sites are altered, which enhances nuclear import and decreases the proteasome mediated degradation. Thus we predict that C terminal mutation will also affect the interaction of S10 and T157 with Akt1 which might increase p27<sup>Kip1</sup> nuclear localization.

## VI. REFERENCE

- [1] Sherr CJ and Roberts JM., "CDK inhibitors: positive and negative regulators of G1-phase progression", *Genes & development*, Vol. 13, pp. 1501-1512, 1999.
- [2] Kamb AC., 1996. "A Cell Cycle Regulator and Cancer", In: Li JJ, Li SA, Gustafsson JA, Nandi S, Sekely LI, editors. *Hormonal Carcinogenesis II*. New York (USA): Springer Verlag, pp. 59-67
- [3] Massague J and Polyak K., "Mammalian anti proliferative signals and their targets", *Current opinion in genetics & development*, Vol. 5, pp. 91-96, 1995.
- [4] Lloyd RV., Erickson LA., Jin L., Kulig E., Xiang Qian X., Cheville JC., Scheithauer BW., "p27kip1: A Multifunctional Cyclin-Dependent Kinase Inhibitor with Prognostic Significance in Human Cancers", *The American journal of pathology*, Vol. 154, pp. 313-323, 1999.
- [5] Porter PL., Malone KE., Heagerty PJ., Alexander GM., Gatti LA., Firpo EJ., Daling JR., Roberts JM., "Expression of cell-cycle regulators p27Kip1 and cyclin E, alone and in combination, correlate with survival in young breast cancer patients", *Nature medicine*, Vol. 3, pp. 222-225, 1997.
- [6] Fredersdorf S., Burns J., Milne AM., Packham G., Fallis L., Gillett CE., Royds JA., Peston D., Hall PA, Hanby AM, Barnes DM, Shousha S, O'Hare MJ, Lu X., "High level expression of p27kip1 and cyclin D1 in some human breast cancer cells: inverse correlation between the expression of p27kip1 and degree of malignancy in human breast and colorectal cancers", *Proceedings of the National Academy of Sciences*, Vol. 94, pp. 6380-6385, 1997.
- [7] Spirin KS., Simpson JF., Takeuchi S., Kawamata N., Miller CW., Koeffler HP., "p27/Kip1 mutation found in breast cancer", *Cancer Research*, Vol. 56, pp. 2400-2404, 1996.
- [8] Russo AA., Jeffrey PD., Patten AK., Massagué J., Pavletich N P., "Crystal structure of the p27Kip1 cyclin-dependent-kinase inhibitor bound to the cyclin A-Cdk2 complex", *Nature*, Vol. 382(6589), pp. 325-331, 1996.
- [9] Wu W I., Voegtli WC., Sturgis HL., Dizon FP., Vigors GP., Brandhuber BJ., "Crystal structure of human AKT1 with an allosteric inhibitor reveals a new mode of kinase inhibition", *PLoS One*, Vol. 5(9), pp. e12913, 2010.
- [10] Zhang Y., ROSETTA server for protein 3D structure prediction. *BMC bioinformatics*, Vol. 9, pp. 40, 2008.
- [11] Kelley LA., Sternberg MJ., "Protein structure prediction on the Web: a case study using the Phyre server", *Nature protocols*, Vol. 4, pp. 363-371, 2009.
- [12] Benkert P., Tosatto SC., Schomburg D., "QMEAN: A comprehensive scoring function for model quality assessment", *Proteins: Structure, Function, and Bioinformatics*, Vol. 71, pp. 261-277, 2008.
- [13] Laskowski RA., MacArthur MW., Moss DS., Thornton JM., "PROCHECK: a program to check the stereochemical quality of protein structures", *Journal of applied crystallography*, Vol. 26, pp. 283-291, 1993.
- [14] Eswar N., Webb B., Marti-Renom MA., Madhusudhan M., Eramian D., Shen My., Pieper U., Sali A., "Comparative protein structure modeling using Modeller", *Current protocols in bioinformatics*, Chapter 5, Unit 5.6, pp. 5.6. 1-5.6. 30 2006.
- [15] De Vries SJ., van Dijk M., Bonvin AM., "The HADDOCK web server for data-driven biomolecular docking", *Nature protocols*, Vol. 5, pp. 883-897, 2010.



- [16] de Vries S.J., Bonvin A.M., "CPORT: a consensus interface predictor and its performance in prediction-driven docking with HADDOCK", *PLoS One*, Vol. 6(3), pp. e17695, 2011.
- [17] Steinberg S.F., "Structural basis of protein kinase C isoform function", *Physiological reviews*, Vol. 88, pp. 1341-1378, 2008.
- [18] Li L., Li C., Sarkar S., Zhang J., Witham S., Zhang Z., Wang L., Smith N., Petukh M., Alexov E., "DelPhi: a comprehensive suite for DelPhi software and associated resources", *BMC biophysics*, Vol. 5, pp. 9, 2012.
- [19] Rodier G., Montagnoli A., Di Marcotullio L., Coulombe P., Draetta G.F., Pagano M., Meloche S., "p27 cytoplasmic localization is regulated by phosphorylation on Ser10 and is not a prerequisite for its proteolysis", *The EMBO journal*, Vol. 20, pp. 6672-6682, 2002.
- [20] Jen J., Harper J.W., Bigner S.H., Bigner D.D., Papadopoulos N., Markowitz S., Willson J.K., Kinzler K.W., Vogelstein B., "Deletion of p16 and p15 genes in brain tumors", *Cancer Research*, Vol. 54, pp. 6353-6358, 1994.
- [21] Shin I., Yakes F.M., Rojo F., Shin N.Y., Bakin A.V., Baselga J., Arteaga C.L., "PKB/Akt mediates cell-cycle progression by phosphorylation of p27Kip1 at threonine 157 and modulation of its cellular localization", *Nature medicine*, Vol. 8, pp. 1145-1152, 2002.
- [22] Muller R.A., Morris D.E., "Geomagnetic reversals driven by sudden climate changes", *Eos*, Vol. 70, pp. 276, 1989.
- [23] Carrano A.C., Eytan, Hershko A., Pagano M., "SKP2 is required for ubiquitin-mediated degradation of the CDK inhibitor p27", *Nature cell biology*, Vol. 1, pp. 193-199, 1999.
- [24] Motti M. L., De Marco C., Califano D., Fusco A., Viglietto G., "Akt-dependent T198 phosphorylation of cyclin-dependent kinase inhibitor p27kip1 in breast cancer", *Cell Cycle*, Vol. 3, pp. 1072-1078, 2004.
- [25] Kozak M., "Recognition of AUG and alternative initiator codons is augmented by G in position+ 4 but is not generally affected by the nucleotides in positions+ 5 and+ 6", *The EMBO journal*, Vol. 16, pp. 2482-2492, 1997.
- [26] Frottin F., Martinez A., Peynot P., Mitra S., Holz R.C., Giglione C., Meinnel T., "The proteomics of N-terminal methionine cleavage", *Molecular & Cellular Proteomics*, Vol. 5, 2336-2349, 2006.
- [27] Moerschell R., Hosokawa Y., Tsunasawa S., Sherman F., "The specificities of yeast methionine aminopeptidase and acetylation of amino-terminal methionine in vivo Processing of altered iso-1-cytochromes c created by oligonucleotide transformation", *Journal of Biological Chemistry*, Vol. 265, pp. 19638-19643, 1990.
- [28] Ponce-Castañeda M.V., Lee M.H., Latres E., Polyak K., Lacombe L., Montgomery K., Mathew S., Krauter K., Sheinfeld J., Massague J., "p27Kip1: chromosomal mapping to 12p12-12p13.1 and absence of mutations in human tumors", *Cancer Research*, 1995; 55: 1211-1214.
- [29] Morosetti R., Kawamata N., Gombart A.F., Miller C.W., Hatta Y., Hiramata T., Said J.W., Tomonaga M., Koeffler H.P., "Alterations of the p27KIP1 gene in non-Hodgkin's lymphomas and adult T-cell leukemia/lymphoma", *Blood*, 1995; 86: 1924-1930.
- [30] Mendelsohn A.R., Brent R., "Protein interaction methods-toward an endgame", *Science*, 1999; 284: 1948-1950.
- [31] Kessel A., Ben-Tal N., "Introduction to proteins: structure, function, and motion", (CRC Press, 2012).